Effects of fillers on the fracture behaviour of particulate polyester composites

K J Wong[1], **B F Yousif**[2*], **K O Low**[1], **Y Ng**[1], and **S L Tan**[1]
[1]Faculty of Engineering and Technology, Multimedia University, Jalan Ayer Keroh Lama, Melaka, Malaysia
[2]Faculty of Engineering, University of Nottingham Malaysia, Jalan Broga, Semenyih, Selangor, Malaysia

Abstract: In the current work, the fracture toughness of sand-particle- and wood-flake-reinforced polyester composites was studied under a linear elastic fracture mechanics approach. The effects of the particulate volume fraction (0–60 vol %) were studied. Scanning electron microscopy was used to observe the damage features on the composite surface. Results showed that sand-particle- and fine-wood-flake-reinforced polymer composites exhibited better results at 40 vol % than at other particulate volume fractions. Meanwhile, coarse-wood-flake-reinforced polymer composites showed higher properties at 30 vol % than at other particulate volume fractions. Observation of the composite surface after tests showed that sand particles have poor interfacial adhesion compared with wood flakes.

Keywords: sand particles, wood flakes, polyester composites, fracture toughness

1 INTRODUCTION

Unsaturated polyester is widely used for pipes, tanks, boat hulls, architectural panels, car bodies, panels in aircraft, and stackable chairs [1, 2]. Many attempts have been made to improve the structural properties of polyester. One of the critical issues in unsaturated polyester is the poor mechanical resistance to cracks because it is difficult to produce flaw-free materials.

To overcome the above problem, reinforcements (particles, fibres, etc.) have been used for polyester. Particulate composites have the advantage of simplicity of fabrication and low cost compared with fibrous and laminate composites [3]. Particulates chosen as reinforcement are usually harder and stiffer than the matrix material. This improves the hardness and stiffness of polymeric composites. However, owing to the limited surface area of contact, the load transfer from matrix to particles occurs to a smaller extent. This could lead to insignificant improvement in strength and impact resistance [3, 4].

Several analyses have been carried out to study the effects of particulates on the mechanical properties of polymeric composites. For example, Zahran [5] studied the effects of sand particle size, shape, and content on the solid state deformation, flow, and fracture behaviour of polyethylene composites. In that work, smaller particles exhibited better reinforcing ability, while larger particles reduced the tensile modulus of the composites and decreased the tensile strength. In other words, sand fillers reduced the yield strength, ductility, and energy absorbed to fracture of the composites. Spanoudakis and Young [6] tested glass-particle-filled epoxy resin and reported that increasing the particle volume fraction increased both Young's modulus and the fracture toughness. Also, increasing the particle size decreased Young's modulus; this was due to the 'skin' effect. As for the fracture toughness, the highest value was obtained at the highest volume fraction of the largest particles. Moloney *et al.* [7] studied the effects of several parameters on the mechanical properties of particulate composites. The results showed that the tensile strength, tensile modulus, flexural strength, flexural modulus, compressive yield strength, and fracture toughness improved with increasing volume fraction of silica particulates. However, the tensile strengths of the composites were always lower than that of the

---

*Corresponding author: Faculty of Engineering, University of Nottingham Malaysia, Jalan Broga, Semenyih 43500, Selangor, Malaysia.
email: belalyousif@yahoo.com; belal.yousif@nottingham.edu.my

neat epoxy when the volume fraction was lower than 50 vol %. Also, larger particle sizes decreased the flexural strength of the composites. Nakamura and Yamaguchi [8] reported that the fracture toughness and energy release rate of spherical-silica-particle-reinforced epoxy composites improved with increasing particle size (between 6 μm and 42 μm). In other research studies [9, 10], it has been reported that increasing the particle size decreased the flexural strength improved the fracture toughness of polymeric composites [10]. Kitey and Tippur [11, 12] have studied the effects of the particle size (7–200 μm) on the dynamic fracture of glass-bead-filled epoxy composites. In that research, the elastic properties were unaffected by the particle size and bonding strength. For untreated particulate composites, the highest fracture toughness was obtained at a particle size of 35 μm. A further increase or decrease in the particle size was found to cause the fracture toughness to deteriorate further.

Mall *et al.* [13] studied the effects of the sand filler size and ductility of polyester on the fracture toughness of particulate composites. The fracture toughness was directly influenced by the matrix ductility. However, the filler size had less effect. Also, Vipulanandan and Dharmarajan [14] studied the fracture behaviour of sand-particle-filled epoxy and polyester composites at various notch depths. The results of that work showed that both epoxy and polyester composites were sensitive to the notch depth. Increasing the polymer content increased the fracture toughness of both epoxy and polyester composites. The impact fracture behaviour of high-density polyethylene (HDPE) composites reinforced with pine wood chips has been studied [15]. It was found that large wood chips with a volume fraction of 50–60 vol % increased the fracture energy of the composites. In contrast, specimens with smaller wood chips absorbed less energy.

Chtourou *et al.* [16] reinforced recycled polyolefins with pulp fibres and reported that the strength and toughness of the composite were increased with the addition of fibre. Sawdust-reinforced post-consumer HDPE composites were studied by Cui *et al.* [17]. The results indicated that wood fibre reinforcement introduced a higher melting point and a slower crystallization rate. Increasing the wood fibre weight fraction increased the flexural strength of the composites. However, a longer fibre length had an adverse effect on the flexural strength. Also, increasing the wood fibre content decreased the Charpy impact strength.

In this study, two types of filler were chosen: sand particles and wood flakes. For wood flakes, two types were selected (fine and coarse flakes). Three different types of particulate composite were fabricated, namely sand-particle-reinforced polyester (SPRP), fine-wood-flake-reinforced polyester (FWFRP), and coarse-wood-flake-reinforced polyester (CWFRP), at different volume fractions. Linear elastic fracture mechanics (LEFM) were adopted to study the fracture behaviour of compact tension (CT) specimens under mode I loading [18].

2 EXPERIMENTAL DETAILS

2.1 Materials

Unsaturated polyester (UP) resin (SYNOLAC 3317AW) was used as resin for the current work and was supplied by Jiashan Anserly Glass Fibre Co. Ltd, Malaysia. Sand particles were obtained from a construction site in Melaka, Malaysia. Sand particles were sieved by a filter net with a mesh size of 1 mm × 1 mm to eliminate rocks and impurities. For impurities smaller than that, it is assumed that the amount is less, thus having insignificant affect on the properties of the composites. This will be further verified in section 3.3 (see Fig. 16(b)). The filtered particles were immersed in water and then washed to clean the surfaces of the particles. This step was repeated five times to ensure cleanliness. After that, the particles were dried for 5 h. The size of the particles was determined using an NJF-1 optical microscope. Ten samples were chosen and the average cross-sectional area was obtained as $0.022 \pm 0.002 \, \text{mm}^2$ (Fig. 1). The sand particles were categorized as fine particles according to the Krumbein [19] scale.
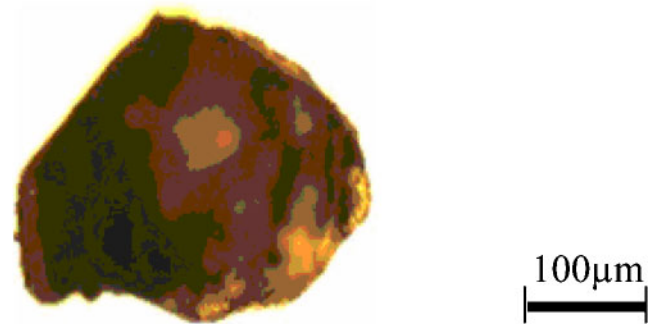

Fig. 1 Average size of the sand particles used in this study

Wood flakes were obtained locally from a wood-manufacturing factory. The wood flakes were a waste product from the sawdust of Chengal (*Neobalano-carpus heimii*) wood pieces. Generally, the wood flakes were categorized as fine (1.2 mm^2) and coarse (7.5 mm^2) (Fig. 2). Table 1 shows some of the physical and mechanical properties of UP, sand particles, and wood flakes.

2.2 Fabrication of samples

Three different types of particulate composite were fabricated at different volume fractions. These composites are SPRP, FWFRP, and CWFRP. The specimens were fabricated using the hand lay-up technique. First, the inner surfaces of a metal mould (the same size as the specimen) were coated with a thin layer of wax as the release agent. The UP resin was mixed with 1 vol % methyl ethyl ketone peroxide catalyst as hardener. Sand particles or wood flakes were added to the mixed resin and poured slowly into the mould. The prepared samples were cured at room temperature for 24 h. Specimens were fabricated with different volume fractions ranging from 0 vol % to 60 vol % for all types of composite, in increments of 10 vol %. The specimens were then sawn with a saw blade of 0.5 mm thickness to initiate sharp precracks.

A schematic diagram of a CT specimen is illustrated in Fig. 3. The dimensions of the specimens were determined according to ASTM D5045-99 [24]. The dimensions of the tensile specimens (Fig. 4) were according to ASTM D638-99 [25], and they were fabricated using a similar procedure to that used for the CT specimens.
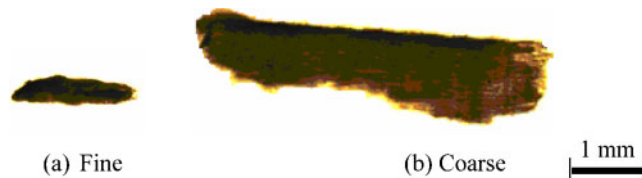

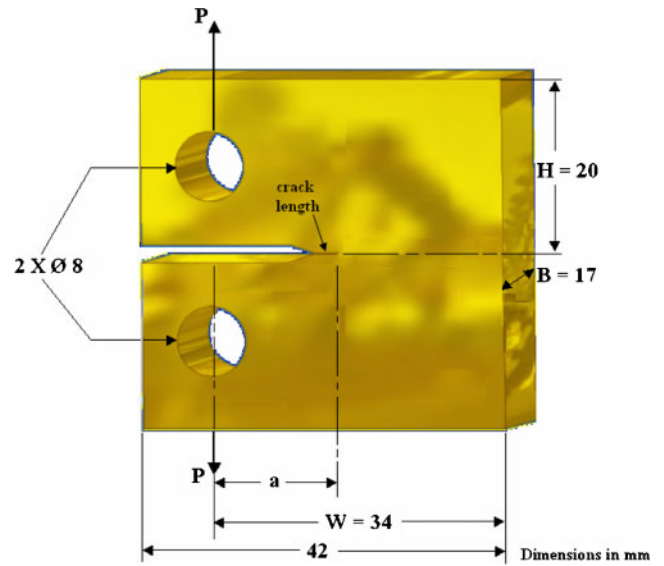**Fig. 2** Average size of the wood flakes used in this study

(a) Fine   (b) Coarse   1 mm

Fig. 3 Schematic diagram of a CT specimen
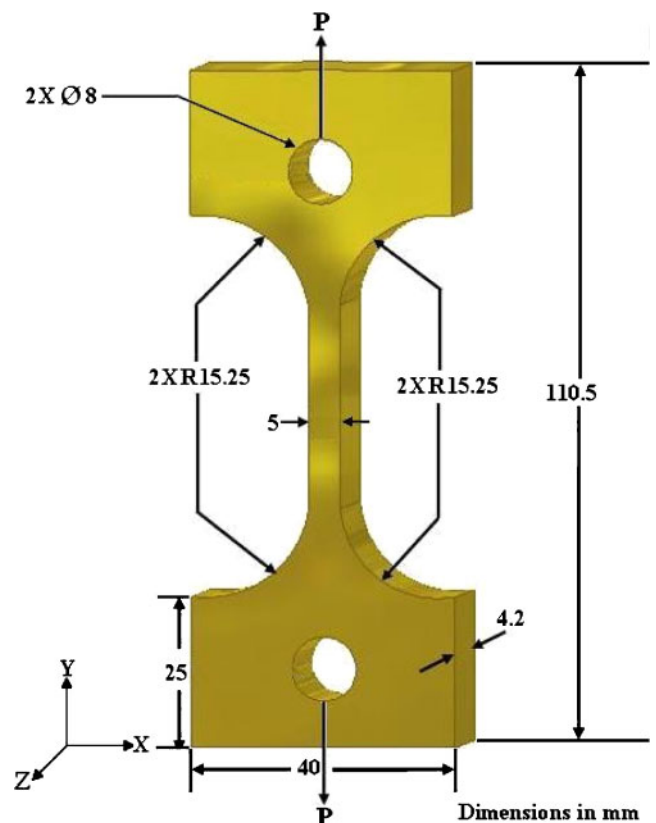

Fig. 4 Schematic diagram of a tensile test specimen

Table 1 Physical and mechanical properties of UP and Chengal wood [20–23]

	Tensile strength (MPa)	Young's modulus (GPa)	Elongation at breaking point (%)	Density (mg/m^3)
UP	50	3.5	2–3	1.2–1.5
Sand	—	73.1	—	—
Chengal wood	149	19.6	—	0.915–0.980

2.3 Experimental procedure

The fracture toughness and tensile tests were conducted using a 100Q stand-alone universal test system according to ASTM D5045-99 and ASTM D638-99 respectively. Tensile tests were conducted to obtain Young's modulus as the input to determine the critical energy release rate. The tests were performed at room temperature, with cross-head speed of 1.5 mm/min for all tests. The precrack for fracture toughness tests was 3 mm. Each test was repeated five times for each type of specimen, and the average values were determined. The load P at breaking point and the corresponding displacement were recorded. The fracture toughness K_{Ic} was calculated using the following equations. The critical stress intensity factor or facture toughness is given by

$$K_{Ic} = \frac{P}{B\sqrt{w}} f\left(\frac{a}{w}\right) \qquad (1)$$

For a CT specimen, the geometry factor $f(a/w)$ is given by

$$f\left(\frac{a}{w}\right) = \frac{2+a/w}{(1-a/w)^{1.5}} \left[0.866 + 4.64\frac{a}{w} - 13.32\left(\frac{a}{w}\right)^2 \right.$$
$$\left. + 14.72\left(\frac{a}{w}\right)^3 - 5.6\left(\frac{a}{w}\right)^4\right] \quad (2)$$

where the relevant parameters are illustrated in Fig. 3.

The particulate composites throughout this study are assumed to be isotropic, which is a similar assumption to that made by Silva *et al.* [18] for short-fibre composites. The assumption is supported by the fact that sand particles are essentially round. Also, thin wood flakes, which are primarily two dimensional, can be assumed to impart equal strength in all directions in their plane [3]. Comparing the current work with the sisal and coconut fibres (1 cm long) used in the work reported in reference [18], coarse wood flakes are considered sufficiently small. Hence, it is assumed that the random distribution of wood flakes does not affect the properties of the composites in different planes.

Also, plane strain applies under the conditions that both neat polyester and glass-fibre-reinforced composites show a linear elastic material response up to the peak load and satisfy the condition

$$B > 2.5 \frac{K_{Ic}^2}{\sigma_{yield}^2} \qquad (3)$$

2.4 Morphology study

The morphology of the fibre and matrix surfaces was studied using scanning electron microscopy (JEOL-JSM 840, Japan). All specimens were gold sputtered using an auto fine coater (JEOL JFC-1600, Japan) before the analysis.

3 RESULTS AND DISCUSSION

3.1 Tensile properties

Figure 5 represents the stress–strain curves of neat polyester and all the composites (SPRP, FWFRP, and CWFRP) at 50 vol % reinforcement. The figure shows relatively linear curves until ultimate failure. This
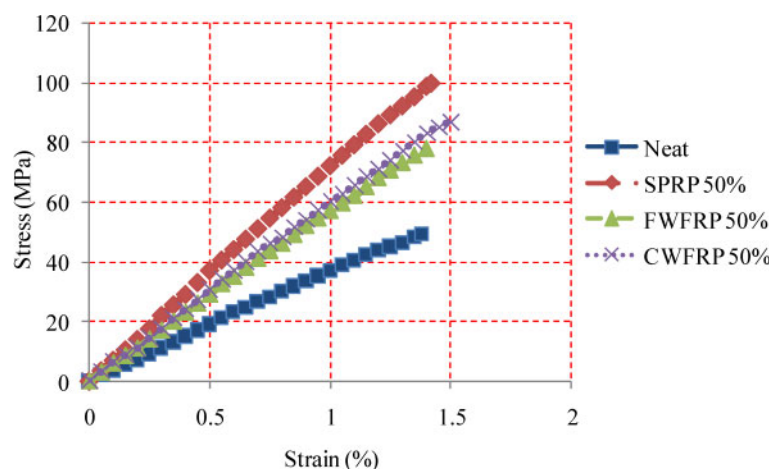

Fig. 5   Stress–strain curves of neat polyester and of SPRP, FWFRP, and CWFRP composites with 50 vol % of reinforcement
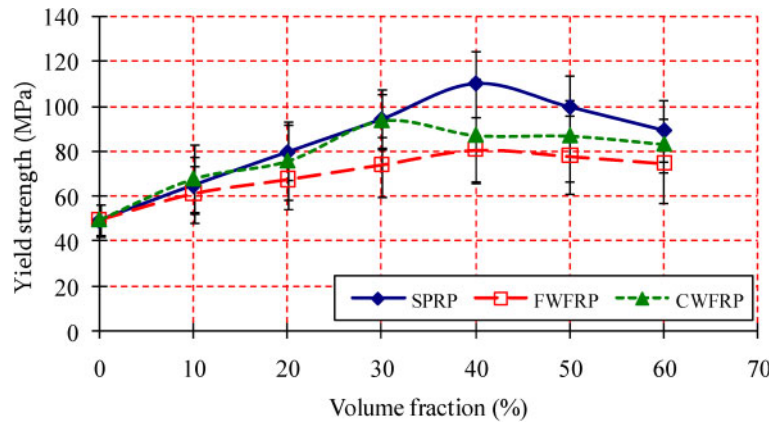
Fig. 6 Yield strength of SPRP, FWFRP, and CWFRP composites with different particulate contents
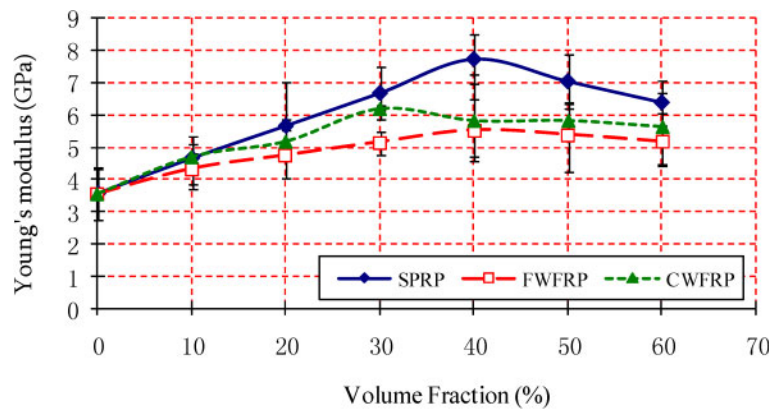

Fig. 7 Young's modulus of SPRP, FWFRP, and CWFRP composites with different particulate contents

indicates that all the materials have a linear elastic and brittle behaviour. Figures 6 and 7 show the effects of the particulate volume fraction on the yield strength and Young's modulus of all types of composite. The average yield strength of neat polyester is about 49 MPa, which is close to the value (50 MPa) established in references [20] and [21]. Young's modulus is about 3.55 GPa, which is similar to the values reported in references [20] and [21]. It can be seen that the highest yield strength is achieved at 40 vol% for SPRP and FWFRP, while 30 vol% for CWFRP exhibits the best result. Regarding the improvement gain in the yield strength of polyester, the maximum is 123 per cent for SPRP, 88 per cent for CWFRP, and 62 per cent for FWFRP. Similar observations are obtained for Young's modulus, i.e. maximum improvements of 117 per cent for SPRP, 75 per cent for FWFRP, and 56 per cent for CWFRP. This could be because the fillers used in this study have better mechanical properties than neat polyester does.

According to Ishai and Cohen [26], the composite modulus of cubic particle composites, for the iso-strain condition, is described by

$$E_c = E_m \left\{ 1 + \frac{V_p}{[m/(m-1) - V_p^{1/3}]} \right\} \tag{4}$$

and, for the iso-stress condition, is given by

$$E_c = E_m \frac{1 + (m-1)V_p^{2/3}}{1 + (m-1)(V_p^{2/3} - V_p)} \tag{5}$$

where

E_c = composite modulus
E_m = matrix modulus
V_p = particulate volume fraction
m = modular ratio (i.e. ratio of the particulate modulus to the matrix modulus)

Equations (4) and (5) with the composite modulus obtained experimentally are plotted together, as
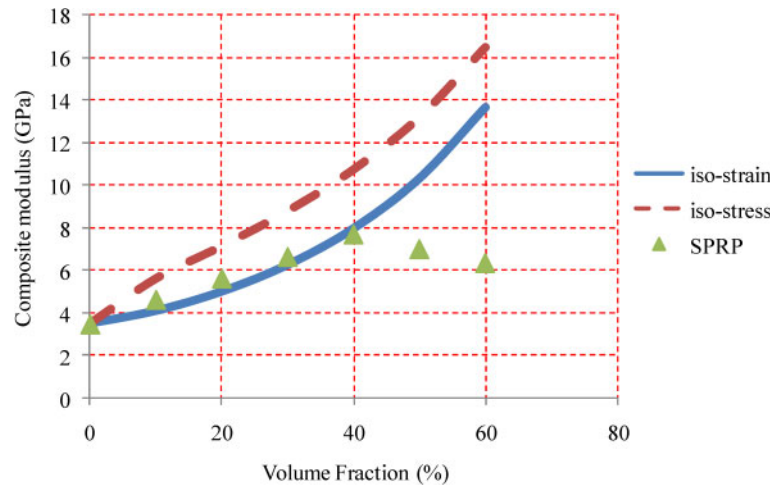
Fig. 8 Variation in the composite modulus with different particulate contents for SPRP composites according to the Ishai–Cohen model
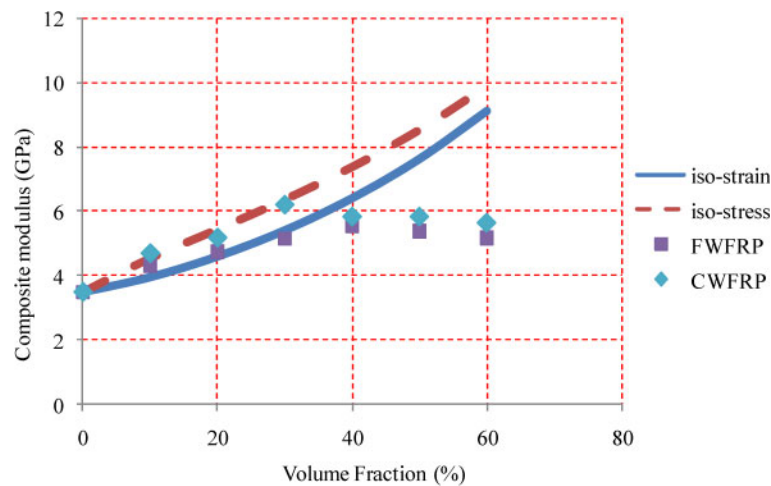

Fig. 9 Variation in the composite modulus with different particulate contents for FWFRP and CWFRP composites according to the Ishai–Cohen model

shown in Figs 8 and 9. From Fig. 8, it is observed that, up to 40 vol % of reinforcement, the experimental data are closer to the iso-strain condition, i.e. the sand particles and surrounding matrix experienced uniform displacement upon loading. Beyond 40 vol %, the experimental data and the theoretical expectation do not have the same trends and values. This could be due to poor interfacial adhesion. Further explanation will be given in section 3.3. In Fig. 9, it seems that, up to 30 vol % reinforcement, the data for FWFRP composites fit the iso-strain condition better, whereas the data for CWFRP composites fit the iso-stress condition better. This suggests that fine wood flakes experience uniform displacement with the matrix nearby, and coarse wood flakes experience uniform stress at the parti-

culate–matrix boundary. However, the upper and lower boundaries are close to each other; hence the difference between them is not significant.

SPRP composites generally showed better properties than WFRP composites did. This indicates that sand particles provide better support in terms of strength and stiffness to neat polyester than wood flakes do. CWFRP composites exhibit better results than FWFRP composites. At the same volume fraction, the quantity of coarse fibres is obviously less than that of fine flakes. Hence, there are fewer surfaces overlapping each other for CWFRP composites, thus increasing the surface area of contact with the matrix for more effective load transfer; this could be the reason for the better performance of CWFRP compared with FWFRP. After the maximum values

of the properties are attained, any further increase in volume fraction weakens the respective properties; this is due to the poor adhesive bonding between the particulates and the polyester resin. Weak bonding weakens the stress transmittance from matrix to particulates. Also, it could be related to the surface property, where a higher particulate content gives a larger area of contact, allowing more skin depletion. Thus, the stiffness of the composites decreases [27].

According to the Hirsch [28] model, the composite modulus with consideration of stress transfer efficiency is given by

$$E_c = \beta\left(E_m V_m + E_p V_p\right) + (1 - \beta)\frac{E_p E_m}{E_m V_p + E_p V_m} \qquad (6)$$

where

E_c = composite modulus
E_p = particulate modulus
E_m = matrix modulus
V_p = particulate volume fraction
V_m = matrix volume fraction
β = stress transfer efficiency factor

The Hirsch model and the experimental data are plotted in Fig. 10. The letters s and w refer to sand particles and wood flakes respectively. It is found that, for SPRP and FWFRP composites, the data are best fitted to the Hirsch model at $\beta = 0.1$. As for CWFRP composites, best fit is at $\beta \approx 0.5$. This indicates that coarse wood flakes have better interfacial adhesion than others. This could be another reason why CWFRP composites have a better strength and stiffness than FWFRP composites do.

Also, the adverse effect of particulate content could also be affected by the surface flaws of the particulates. Surface flaws could be introduced by rubbing and abrading the particulate surfaces with another material from the fabrication of previous composites. As the volume fraction of particles increases, the probability of surface flaws increases. It has been reported that flaws could easily be generated during testing by microvoid coalescence or plastic deformation of a certain region of the specimen [7]. Therefore, the increase in the strength caused by the increase in the volume fraction of particles was offset by the decrease in the strength caused by the increase in the number of surface flaws.

3.2 Fracture properties

Figure 11 represents the load–displacement curves of neat polyester and all types of composite at 50 vol %. The curves show relatively linear elastic behaviour, with a slight upward curve observed for the composites. Once the peak load is attained, it is accompanied by a sudden drop. No zigzag behaviour is noticed in any of the curves; hence it is expected that the crack growth occurred in a steady state fashion. With these observations, one of the criteria of LEFM is satisfied.

The fracture toughness is calculated using equations (1) and (2); the geometry and the load P at failure were obtained experimentally. Figure 12 shows the fracture toughness of different types of composite at different particulate contents. As the volume fraction increases, the fracture energy and
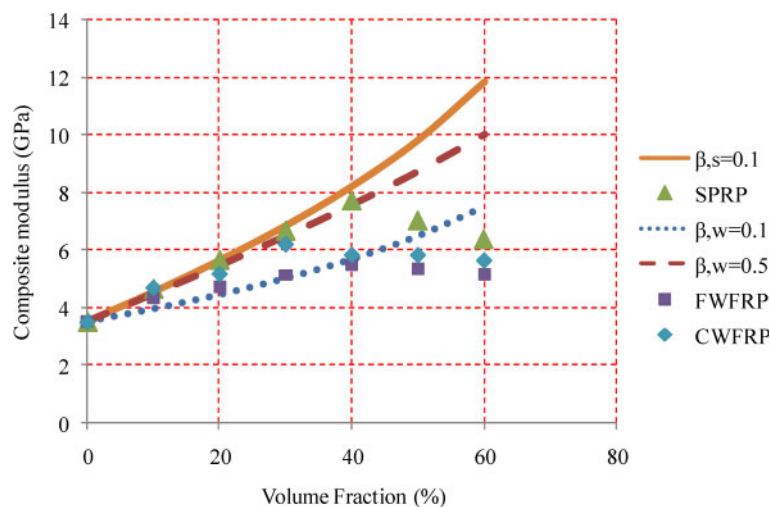

Fig. 10 Variation in the composite modulus with different particulate contents for FWFRP and CWFRP composites according to the Hirsch model
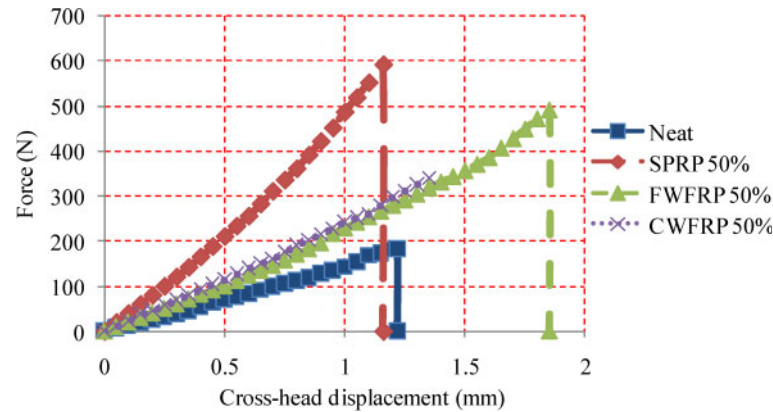
Fig. 11 Load–displacement curves of neat polyester and of SPRP, FWFRP, and CWFRP composites with 50 vol % of reinforcement
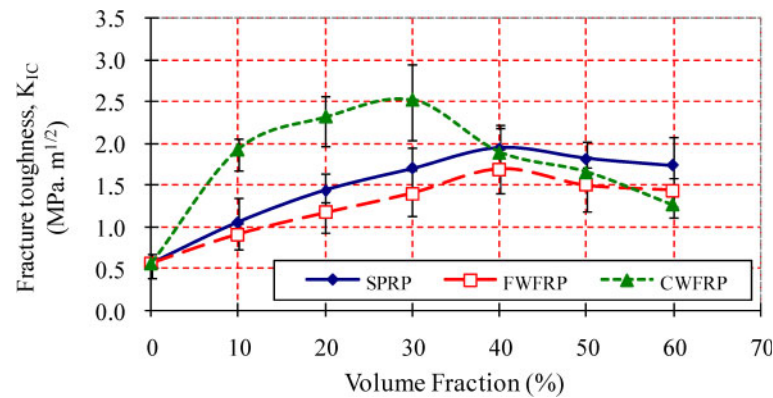

Fig. 12 Fracture toughness of SPRP, FWFRP, and CWFRP composites at different particulate contents

damage resistance of the composites increases, which can be observed through the improvement in the fracture toughness. Similar to the tensile properties, the maximum fracture toughness is exhibited at 40 vol % for SPRP and FWFRP composites, and at 30 vol % for CWFRP composites. Similar results have been reported by Spanoudakis and Young [6], where increasing the volume fraction increased the fracture toughness. The most generally accepted reason for this result is crack front pinning. This is due to the obstructions to the propagation of the crack front by the particulates and causes the primary cracks to bow out between the particulates, which forms secondary cracks and leads to an
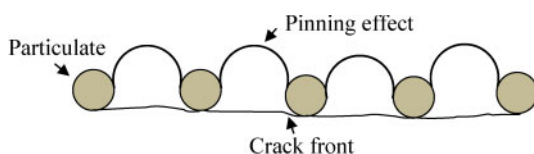
increase in the toughness [29]. Figure 13 describes this schematically. However, this fracture mechanism is only suitable for low volume fractions. As the volume fraction increases, there could be considerable breakdown of the particulate–matrix interface, i.e. causing pinning is more difficult [11]. Another fracture mechanism is crack tip blunting, where the crack growth is retarded because of particulate debonding (Fig. 14). Thus, this is expected for composites at high particulate contents, i.e. the fracture toughness is still increasing because of higher blunting. Similar observations have been reported by Owen [30] and Su and Suh [31], where debonding of particulates gave rise to crack tip blunting and unstable propagation. However, this is
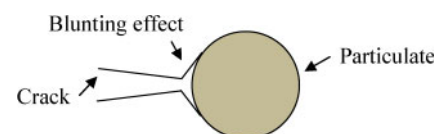

Fig. 13 Schematic representation of crack front pinning

Fig. 14 Schematic representation of crack tip blunting

not always true, as shown by the experimental results. Beyond the optimum fibre content, a further increase in the volume fraction has an adverse effect on the fracture toughness (Fig. 12). Hence, there must be another mechanism for it.

This could be due to poorly bonded particulates that link up to create larger flaws [7]. Hence, the fracture toughness decreases as the particulate content increases beyond the optimum value. Also, Kitey and Tippur [12] proposed that crack front twisting is the reason for this. For weak bonding, the crack front goes through the particulates or particulate footprints. These form tail lines between particulates, which indicate the crack propagation direction as described in Fig. 15. Gradually, the crack front is twisted until it reaches the maximum angle ϕ_{max}. Beyond this, tail lines emerge from two neighbouring particulate sites. This creates an additional surface, dissipates additional energy, and affects the surface features as well. It is suggested that crack twisting happens more often at weak interfaces.

At low particulate contents, the separation between particulates is larger, hence increasing the probability that the crack travels through matrix material. This in turn decreases the average value of ϕ. On the other hand, at higher particulate contents, there is a larger number of particulates per unit volume, i.e. the separation between particulates is less. This reduces the difference in the elevations between particulates during propagation, which in turn reduces ϕ as well. Neither condition contributes to increasing the fracture toughness of the composites. The average ϕ is near or equal to ϕ_{max} at optimum particulate content for each type of composite, where the failure is primarily due to crack twisting.

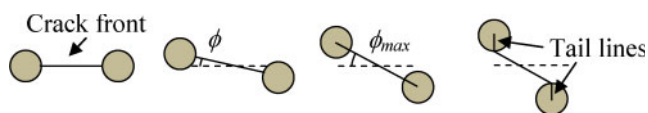The results show that CWFRP composites exhibit better fracture toughness than FWFRP composites

Fig. 15 Schematic representation of crack front twisting [12]

do. This could be due to the difference in the sizes of the wood flakes used in this study. It has been reported that there is an optimum particulate size to obtain the highest fracture toughness [11]. An increase or decrease in the particulate size decreases the fracture toughness. Hence, it is proposed that coarse wood flakes have a size that is closer to the optimum value. However, it was not determined that the coarse wood flakes used in this study are at the optimum size since only two different sizes of wood flakes were tested. It is recommended that further experimental work is carried out on wood flakes of different sizes.

In addition, SPRP composites show lower fracture resistance than CWFRP composites do at a lower volume fraction of 40 vol %. This could be due to the size effect, where larger particulate surfaces allow cracks to be deflected more effectively. This requires more energy to be dissipated by friction and thus results in a higher fracture energy. A larger chip size could restrict the deformation of the specimen, inducing internal frictional forces [15]. Energy dissipation, through fibre debonding, can also delay the crack growth owing to the decrease in the driving force at the crack tip [32, 33].

To verify further that the plane strain condition applies according to equation (3), calculations were carried out as shown in Table 2, which demonstrates that all types of composite are thick enough (16 mm) to satisfy the plane strain condition.

3.3 Morphology study

Fracture surfaces of different tested materials are given in Fig. 16. The micrographs show that there is no agglomeration for all types of composite including neat polyester. In neat polyester, the crack surface is uniform along the crack path. Moreover, cracks propagate directly and there is no retardation in crack growth. This indicates the brittle behaviour of the material, and there is no plasticity observed before final failure. According to LEFM theory, when the energy is sufficient to initiate crack growth for a typical brittle material, catastrophic failure occurs, and there is no crack deflection.

Table 2 Verification of specimen thicknesses for the plane strain condition

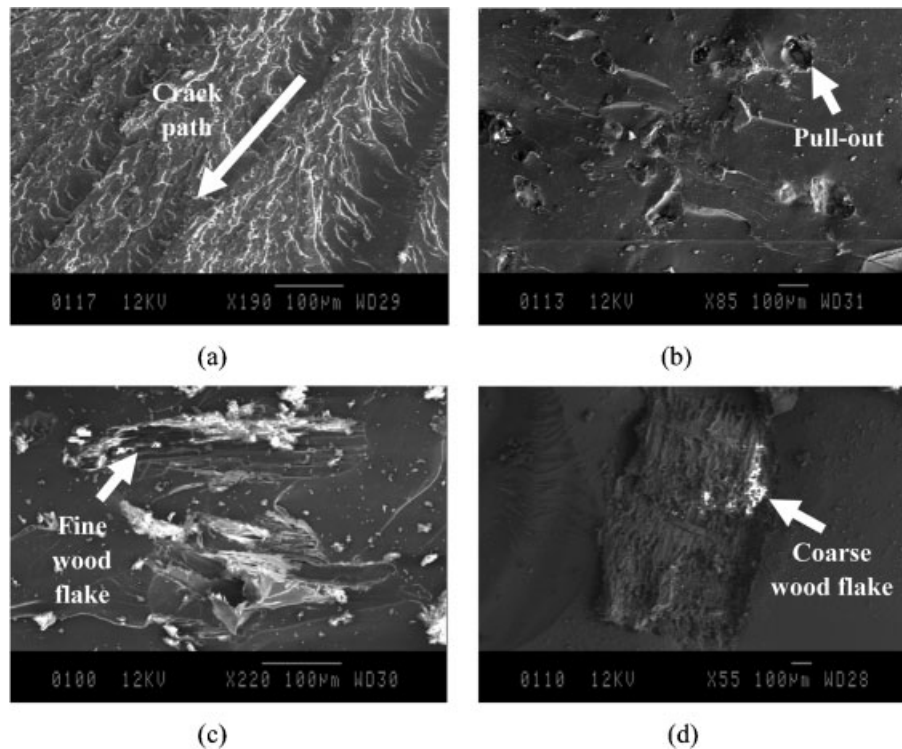|	Specimen thickness (mm) for the following volume fractions						
	0 vol %	10 vol %	20 vol %	30 vol %	40 vol %	50 vol %	60 vol %
SPRP	0.32	0.66	0.81	0.82	0.78	0.83	0.94
FWFRP	0.32	0.55	0.75	0.89	1.10	0.93	0.92
CWFRP	0.32	2.01	2.33	1.82	1.18	0.90	0.57

Fig. 16   Fracture surfaces of (a) neat polyester, (b) SPRP composite with 50 vol % reinforcement, (c) FWFRP composite with 50 vol % reinforcement, and (d) CWFRP with 50 vol % reinforcement

For the composites, as the crack reaches the particulate–matrix interface, the crack either breaks the particulate or is deflected along the interface, which causes debonding. The mechanism strongly depends on the bonding between the particulate and the matrix. If the particulate strength is greater than interfacial shear strength, the particulate is pulled out before it is broken and vice versa. For better fracture toughness, weaker interfacial adhesion is desirable. This is because, as the crack is deflected, energy is dissipated along the interface. This slows down the crack growth rate and leads to a tortuous crack path [18].

Figure 16(b) shows the fracture surface of a 50 vol % SPRP composite. Holes can be observed on the surface, indicating particles that have been pulled out from the matrix. The sizes of the holes are similar to the particle sizes. This confirms the poor particle–matrix interface bonding, where the maximum tensile stress is at the equators of particles and holes [34, 35]. Hence, a crack is propagated around the equators. Thus, the micrograph shows a surface that consists of hemispherical holes and the top surface of debonded particles. As the crack front intersects the interface, the matrix surrounding the filler is separated owing to weak bonding. It is observed that the crack front bows out wherever it

interacts with the particles: i.e. the crack tip is being blunted at discrete locations along the crack front. The crack tip blunting is due to particle debonding, which retards the crack growth and lowers the stress intensification [11, 12]; this takes place through localized shear yielding [36, 37]. In addition, it is suggested that the high toughness is due to debonding of particles that act as voids, causing more localized energy-absorbing processes, such as plastic deformation [38]. Also, additional energy is needed to overcome blunting for crack re-initiation and further propagation. This reduces the energy released for crack re-initiation, leading to microcrack formation. Thus, the total dissipated energy is consumed in crack propagation and the formation of localized microcracks. Both phenomena increase the fracture toughness.

Furthermore, interparticle cleavage fracture can be observed, which is characterized by the presence of 'river lines'. On the surface, particles or particle footprints are found left behind. The formation of tail lines between the particles or cavities, which is believed to be due to crack twisting, implied the crack propagation direction [12].

As for FWFRP and CWFRP, particulates are found to be strongly bonded with the resin (Figs 16(c) and (d)). For FWFRP, the blunting effect and tail lines can

be observed (Fig. 16(c)). As for CWFRP composite, crack tip blunting is obviously observed (Fig. 16(d)). However, this does not mean that there is no twisting effect because, for better bonding ($\beta = 0.5$ as discussed earlier), cracks propagate above or below particulate poles through the matrix [**38**]. Hence, the particulates and the tail lines are not distinct. The better interfacial adhesion of wood flakes to polyester is less likely due to the porosity of the wood flakes which allows resin to seep into the flakes and bond well with the resin because of sufficiently high lignin amount [**39–41**].

The observations on the micrographs can be further verified through the experimental results. Comparing the fracture toughnesses of SPRP, FWFRP, and CWFRP at 50 vol % (Fig. 12), SPRP has the highest fracture toughness, followed by CWFRP, whereas FWFRP has the lowest fracture toughness. This is in agreement with the suggestion that poorer interfacial adhesion leads to higher fracture toughness. As for CWFRP, this could also be due to the larger surface area, which allows more energy to be dissipated along the interface, hence leading to higher fracture toughness than for FWFRP.

4 CONCLUSIONS

Based on the work carried out in this study, the following conclusions can be drawn.

1. The maximum tensile strength, Young's modulus, and fracture toughness are obtained at a volume fraction of 40 vol % for SPRP and FWFRP composites, while 30 vol % is the optimum for CWFRP composites. Hence, the corresponding volume fractions are suggested to achieve optimum performance of the respective composites.
2. SPRP composites are stronger and stiffer than other composites. Meanwhile, CWFRP composites are better in terms of fracture resistance.
3. A surface morphology study shows that sand particles have poorer interfacial adhesion than wood flakes do.

© Authors 2010

REFERENCES

1 **Philip, M.** and **Bolton, W.** *Technology of engineering materials*, 2002 (Butterworth–Heinemann, Oxford).
2 **Groover, M. P.** *Fundamentals of modern manufacturing*, 2002 (John Wiley, New York).
3 **Agarwal, B. D., Broutman, L. T.,** and **Chandrashekhara, K.** *Analysis and performance of fibre composites,* 3rd edition, 2006 (John Wiley, New York).
4 **Mallick, P. K.** *Fibre-reinforced composites: materials, manufacturing, and design*, 1993 (Marcel Dekker, New York).
5 **Zahran, R. R.** Effect of sand addition on the tensile properties of compression moulded sand/polyethylene composite system. *Mater. Lett.*, 1998, **34**(3–6), 161–167.
6 **Spanoudakis, J.** and **Young, R. J.** Crack propagation in a glass particle filled epoxy resin. Part 1. Effect of particle volume fraction and size. *J. Mater. Sci.*, 1984, **19**, 473–486.
7 **Moloney, A. C., Kausch, H. H., Kaiser, T.,** and **Beer, H. R.** Review – parameters determining the strength and toughness of particulate filled epoxide resins. *J. Mater. Sci.*, 1987, **22**, 381–393.
8 **Nakamura, Y.** and **Yamaguchi, M.** Effects of particle size on the fracture toughness of epoxy resin filled with spherical silica. *Polymer*, 1992, **33**(16), 3415–3426.
9 **Nakamura, Y., Okabe, S.,** and **Iida, T.** Effects of particle shape, size and interfacial adhesion on the fracture strength of silica-filled epoxy resin. *Polym. Polym. Composites*, 1999, **7**(3), 177–186.
10 **Imanaka, M., Takeuchi, Y., Nakamura, Y., Nishimura, A.,** and **Iida, T.** Fracture toughness of spherical silica-filled epoxy adhesives. *Int. J. Adhesion Adhes.*, 2001, **21**(5), 389–396.
11 **Kitey, R.** and **Tippur, H. V.** Role of particle size and filler–matrix adhesion on dynamic fracture of glass-filled epoxy. I. Macromeasurements. *Acta Mater.*, 2005, **53**, 1153–1165.
12 **Kitey, R.** and **Tippur, H. V.** Role of particle size and filler–matrix adhesion on dynamic fracture of glass-filled epoxy. II. Linkage between macro- and micro-measurements. *Acta Mater.*, 2005, **53**, 1167–1178.
13 **Mall, S., Newaz, G. M.,** and **Farhadinia, M.** Effect of filler size and matrix properties on fracture toughness of particulate composites. *J. Reinf. Plast. Composites*, 1987, **6**, 138–152.
14 **Vipulanandan, C.** and **Dharmarajan, N.** Fracture properties of particle filled polymer composites. *J. Composite Mater.*, 1989, **23**, 846–860.
15 **Razi, P. S.** and **Raman, A.** Studies on impact fracture properties of wood–polymer composites. *J. Composite Mater.*, 2000, **34**, 980–997.
16 **Chtourou, H., Riedl, B.,** and **Ait-Kadi, A.** Reinforcement of recycled polyolefins with wood fibres. *J. Reinf. Plast. Composites*, 1992, **11**, 372–394.
17 **Cui, Y. H., Tao, J., Noruziaan, B., Cheung, M.,** and **Lee, S.** DSC analysis and mechanical properties of wood–plastic composites. *J. Reinf. Plast. Composites*, November 2008, Online first. DOI: 10.1177/0731684408097766.
18 **Silva, R. V., Spinelli, D., Bose Filho, W. W., Claro Neto, S., Chierice, G. O.,** and **Tarpani, J. R.** Fracture toughness of natural fibres/castor oil

polyurethane composites. *Composites Sci. Technol.*, 2006, **66**(10), 1328–1335.

19 **Krumbein, W. C.** and **Sloss, L. L.** *Stratigraphy and sedimentation,* 2nd edition, 1963 (Freeman, San Francisco, California).

20 **Dorf, R. C.** *The engineering handbook*, 1996 (CRC Press, New York).

21 **Hull, D.** and **Clyne, T. W.** *An introduction to composite materials*, 1996 (Cambridge University Press, Cambridge).

22 **Spanoudakis, J.** *Fracture in particle-filled epoxy resins*. PhD Thesis, University of London, London, UK, 1981.

23 Malaysian Timber Council, Specifications of popular Malaysian timber: general properties, 4 August 2008, available from http://www.mtc.com.my/industry/index.php?option=com_content&view=article&id=74&Itemid=61.

24 ASTM D5045-99 *Standard test methods for plane-strain fracture toughness and strain energy release rate of plastic materials*, 1999 (ASTM International, West Conshohocken, Pennsylvania).

25 ASTM D638-99 *Standard test method for tensile properties of plastics*, 1999 (ASTM International, West Conshohocken, Pennsylvania).

26 **Ishai, O.** and **Cohen, L. J.** Elastic properties of filled and porous epoxy composites. *Int. J. Mech. Sci.*, 1967, **9**, 539–546.

27 **Lewis, A. G.** and **Nielsen, L. E.** Dynamic mechanical properties of particulate-filled composite. *J. Appl. Polym. Sci.*, 1970, **14**, 1449–1471.

28 **Hirsch, T. J.** Modulus of elasticity of concrete affected by elastic moduli of cement paste matrix and aggregate. *J. Am. Concr. Inst.*, 1962, **59**, 427–451.

29 **Lange, F. F.** The interaction of a crack front with a second phase dispersion. *Phil. Mag.*, 1970, **22**, 983–992.

30 **Owen, A. B.** Direct observations of debonding at crack tips in glass bead-filled epoxy. *J. Mater. Sci.*, 1979, **14**, 2521–2523.

31 **Su, K. B.** and **Suh, N. P.** Void nucleation in particulate-filled polymeric materials. In Proceed-ings of the Annual Technical Conference of the Society of Plastics Engineers (*ANTEC 81*), Boston, Massachusetts, USA, 1981, Vol. 27, pp. 46–48 (Society of Plastics Engineers, Newtown, Connecticut).

32 **Matthews, F. L.** and **Rawlings, R. D.** *Composite materials: engineering and science*, 1994 (Chapman & Hall, London).

33 **Botsis, J.** and **Beldica, C.** Strength characteristics and fatigue crack growth in a composite with long aligned fibres. *Int. J. Fracture*, 1995, **69**(1), 27–50.

34 **Khaund, A. K., Krstic, V. D.,** and **Nicholson, P. S.** Influence of elastic and thermal mismatch on the local crack-driving force in brittle composites. *J. Mater. Sci.*, 1977, **12**, 2269–2273.

35 **Goodier, J. N.** Concentration of stress around spherical and cylindrical inclusions and flaws. *J. Appl. Mech.*, 1933, **1**, 39–44.

36 **Yamini, S.** and **Young, R. J.** The mechanical properties of epoxy resins. Part 2. Effect of plastic deformation upon crack propagation. *J. Mater. Sci.*, 1980, **15**, 1823–1831.

37 **Kinloch, J. G.** and **Williams, A. J.** Crack blunting mechanisms in polymers. *J. Mater. Sci.*, 1980, **15**, 987–996.

38 **Spanoudakis, J.** and **Young, R. J.** Crack propagation in a glass particle filled epoxy resin. Part 2. Effect of particle-matrix adhesion. *J. Mater. Sci.*, 1984, **19**, 487–496.

39 **Sarkanen, K. V.** and **Ludwig, C. H.** *Lignins: occurrence, formation, structure, and reactions*, 1971 (Wiley–Interscience, New York).

40 **Wong, A. H. H.** *Susceptibility to soft rot in untreated and copper–chrome–arsenic treated Malaysian hard-woods*. PhD Thesis, University of Oxford, Oxford, UK, 1993.

41 **Singh, A. P., Wong, A. H. H., Kim, Y. S., Wi, S. G.,** and **Lee, K. H.** Soft rot decay of cengal (*Neobal-anocarpus heimii*) heartwood in ground contact in relation to extractive microdistribution. Document IRG/WP 03-10501, International Research Group on Wood Preservation, Stockholm, Sweden, 2003.